# Flywheel Energy Storage System with Homopolar Electrodynamic Magnetic Bearing*

Alexei Filatov and Patrick McMullen
*CALNETIX*
*12880 Moore Street*
*Cerritos, CA 90703, USA*
*afilatov@calnetix.com*

Kent Davey and Richard Thompson
*Center for Electromechanics, University of Texas*
*10100 Burnet Road, Bldg. 133*
*Austin, TX 78721-0668, USA*
*k.davey@mail.utexas.edu*

***Abstract* – The goal of this research was to evaluate the potential of homopolar electrodynamic magnetic bearings for flywheel energy storage systems (FESSs). The primary target was a FESS for Low Earth Orbit (LEO) satellites, however, the design can also be easily adapted for Earth-based applications. The main advantages of Homopolar Electrodynamic Bearings compared to more conventional Active Magnetic Bearings (AMB) are simplicity and very low power ratings of their electronics. These result in higher system reliability, which is a critical factor for space applications. For commercial applications, these technologies may equally be found very attractive due to a potentially lower cost when compared to AMB.**

***Index Terms* – Homopolar Electrodynamic Magnetic Bearing, Flywheel.**

## I. INTRODUCTION

The main purpose of an energy storage system in a LEO satellite is to supply power when the solar battery array is non-operational because the satellite is in the Earths' shadow. A typical LEO satellite circles the Earth in approximately 90 minutes and can rely on solar energy for only slightly more than half of this time. A satellite's energy storage system undergoes roughly 60,000 charge/discharge cycles over ten years, well above the endurance limit of a typical electrochemical battery.

A FESS stores energy in the form of kinetic energy of a spinning mass. Energy transformations from electrical into mechanical and back are carried out by an electrical motor/generator. Potentially, a FESS can offer an essentially unlimited number of charge/discharge cycles. Furthermore, if magnetic bearings and a brushless motors/generator are used, the rotor can be suspended without any mechanical contact. This allows very high rotational speeds and energy densities without affecting the system life.

The two important requirements for a satellite FESS are reliability and energy storage density, either per unit weight or volume. With the elimination of mechanical wear, useful operation and performance life is dictated by the reliabilities of the components, particularly the magnetic bearings and the motor/generator. Since the component reliability is directly related to its complexity, a simpler design of the homopolar electrodynamic bearings is an advantage over active magnetic bearings.

## II. FESS DESIGN

### *A. Overall Layout*

A schematic layout of the proposed FESS is shown in Fig. 1. Most of the flywheel's kinetic energy is stored in the composite rim. The aluminium hub connects the rim to the other members of the rotor assembly and also serves as a part of the magnetic bearing in tandem with a stationary magnetic system. This system generates a circumferentially uniform but radially non-uniform magnetic field within the hub. Whenever the hub rotation axis is displaced from the field symmetry axis, eddy currents are induced in its volume, interacting with the field and producing an electromagnetic force with a radial component acting against the displacement. This is the operating principle of a homopolar electromagnetic bearing. Various implementations of this principle have already been described in the literature [1-4].

It is known that a homopolar electromagnetic bearing cannot be stable without an additional component - a damper, which suppresses low-speed whirl motions of the rotor [2, 3]. The damper can be as simple as a set of permanent magnets mounted on the rotor interacting with stationary conductors [5], in which case a completely passive suspension with no electronics will be realized, however, an active damper with some simple electronics has an advantage of lower weight and volume.

An iron-less axial-flux motor/generator is selected in order to minimize disturbing forces on the rotor. The axial suspension is achieved by introducing several stationary magnets interacting with the rotating magnets of the radial damper. Positive angular stiffness is realized by means of two sets of the mutually attractive magnets located at the ends of the machine. Some intermediate results of this development as well as alternative design and analysis solutions not included in this paper can be found in [5].

* This work was performed under NASA contract number NNC04CA97C.

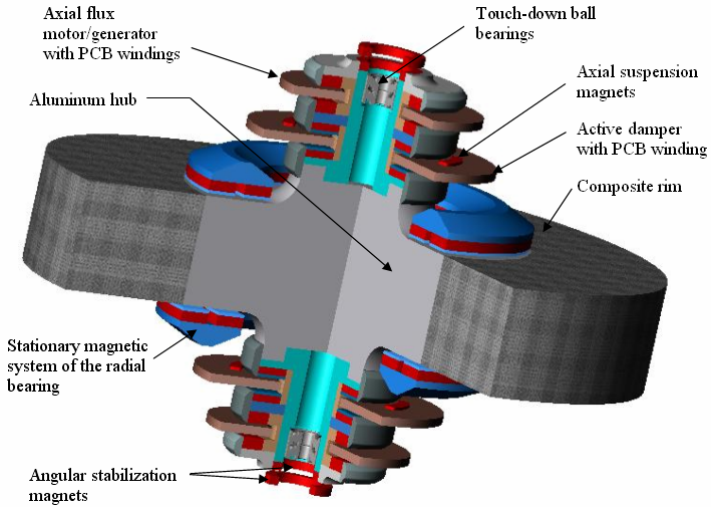


Fig. 1 Schematic layout of the proposed Flywheel Energy Storage System with homopolar electrodynamic magnetic bearings.

### *B. Hub-Rim Assembly*

The amount of stored energy is limited by the stresses in the rotor, primarily in the aluminium hub. The difficulty of the hub design was in part caused by its dual role as a structural member of the flywheel and an element of the magnetic bearing. Several different geometries of the aluminium hub have been evaluated.

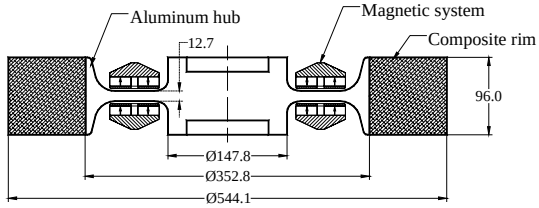


Fig. 2. Variant of the aluminum hub with 12.7 mm axial thickness in the magnetic gap area.

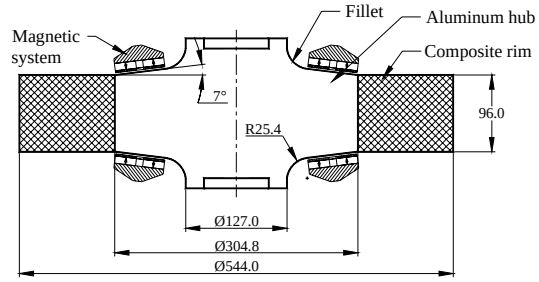


Fig. 3. Variant of the aluminum hub with 96 mm minimal axial thickness in the magnetic gap area.

The variant shown in Fig. 2 is favourable for the magnetic bearing operation because of a relatively low electromagnetic gap and consequently higher magnetic flux density and suspension stiffness. However, the variant shown in Fig. 3 exhibits lower stresses and, therefore, will have a longer cycle life. This variant was found preferable for the satellite FESS application.

For the design shown in Fig. 3, two stress concentration sites were observed in the centre of the hub and on the fillet. Table 1 summarizes the stress components in these locations under different operating speeds and room temperature. The table also includes radial stresses at the rim/hub interface shown in the last column. Keeping these stresses close or below 140 MPa was important to minimize creep in the composite material.

A fatigue analysis has been carried assuming aluminium alloy 7075-T6 as a hub material with 503 MPa tensile yield strength and 572 MPa ultimate strength. The number of cycles-to-failure was estimated as 158,000 cycles, with the rotor speed changing from 15,000 to 35,000 RPM and back again within each cycle. The lower speed limit was chosen as nonzero because under real operating conditions the flywheel is not supposed to slow down below the speed when the generator is not capable of delivering the required power (15 kRPM in our case).

**TABLE 1: STRESS SUMMARY**

**At Rest**

| Stress\Location | Fillet | Center | Interface |
|---|---|---|---|
| Radial | -180 MPa | -124 MPa | -159 MPa |
| Tangential | -138 MPa | -124 MPa | |
| Axial | -48 MPa | 41 MPa | |
| Von-Misses | 165 MPa | 165 MPa | |

**At 15 kRPM**

| Stress\Location | Fillet | Center | Interface |
|---|---|---|---|
| Radial | -103 MPa | -48 MPa | -138 MPa |
| Tangential | -69 MPa | -48 MPa | |
| Axial | 28 MPa | 28 MPa | |
| Von-Misses | 96 MPa | 69 MPa | |

**At 35 kRPM**

| Stress\Location | Fillet | Center | Interface |
|---|---|---|---|
| Radial | 255 MPa | 303 MPa | -41 MPa |
| Tangential | 221 MPa | 303 MPa | |
| Axial | 62 MPa | -48 MPa | |
| Von-Misses | 248 MPa | 359 MPa | |

A more in-depth analysis is still needed to take into account effects of the temperature variations, which are known to be a problem for integration of composite materials with metals due to the large difference of their thermal expansion coefficients. A flywheel design for wide operational temperature range incorporating a composite rim and aluminium hub is described for example in [6]. Even though the direct application of the approach described in [6] would require us to abandon the idea of using the aluminium hub as a part of the magnetic bearing, a separate aluminium disks can be added on two sides of the aluminium hub, dedicated to the bearing function. The majority of the electromagnetic analysis results presented in the following section will still be applicable in this case.

### *C. Homopolar Electrodynamic Radial Magnetic Bearing*

- Generating positive radial stiffness

Positive suspension stiffness in all directions is a necessary condition for suspension stability. It is known from Earnshaw's theorem [7] with subsequent extension by Braunbek [8] that this condition cannot be satisfied by relying only on permanent magnets and permeable materials. In the present system, the net positive stiffness is achieved by utilizing an aluminium hub spinning in a circumferentially uniform magnetic field produced by the magnetic system shown in Figs. 1-3. At first, this stiffness was calculated for the 12.7mm-thick hub (Fig. 2). The main dimensions and other parameters used in the analysis are shown in Fig. 4. The system was "unrolled" for simplicity. The analysis was carried out using 2D FEA program FEMM (http://femm.foster-miller.com). A more accurate method of analysing homopolar electromagnetic bearings using 3D FEA is described in [4]. Fig. 5 shows the static magnetic field distribution. Fig. 6 shows the axial distribution of the axial field component in the middle of one of the poles, which is fairly uniform. Fig. 7 shows radial distribution of the axial field component averaged over the disk thickness along with a similar distribution calculated for the disk shifted by 2.5 mm (the coordinates are measured in the disk coordinate frame).

In order to calculate eddy currents induced in the disk, a harmonic field perturbation was introduced at the magnet boundaries with a frequency equal to the rotational frequency of the disk. The amplitude of the field perturbation was approximately equal to the difference between the field values in Fig. 7 corresponding to the central and displaced disk positions (see Fig. 8).

Eddy currents induced in the aluminium disk during the rotation suppress the external field variation by producing counter-field. The large amplitude of the external field variation (up to 0.2 T with 2.5 mm disk displacement)

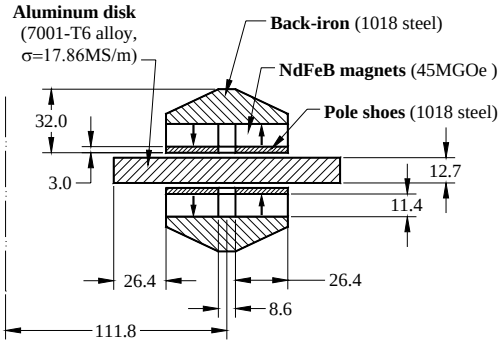


Fig. 4. Parameters of the system used to calculate electromagnetic stiffness produced by the 12.7mm-thick aluminium disk.

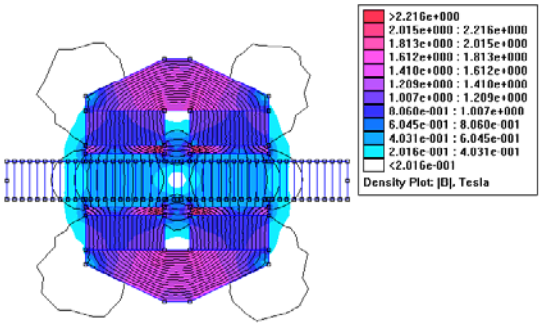


Fig. 5. Static magnetic field distribution for the system shown in Fig.4. The system is "unrolled" to simplify the analysis.

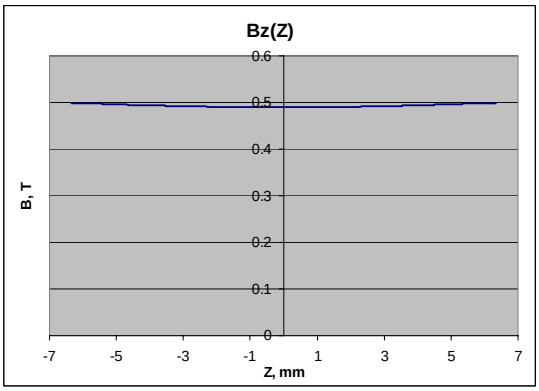


Fig. 6. Axial distribution of the axial field component in Fig.5 (12.7mm-thick disk) in the middle plane of one of the poles.

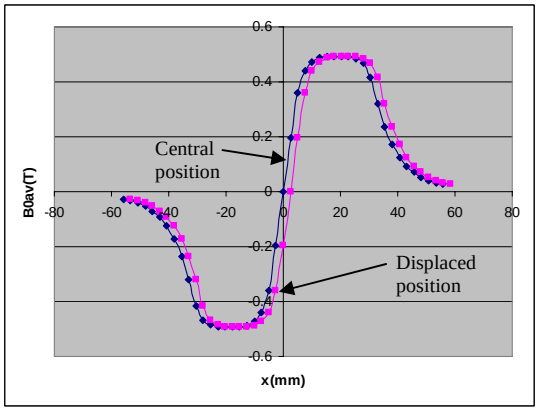


Fig. 7. Axial component of the magnetic field generated by the magnetic system shown in Fig. 4, averaged over the disk thickness.

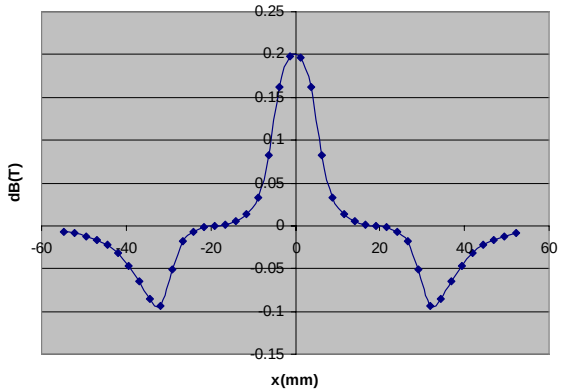


Fig. 8. Change of the axial component of the magnetic field when its axis is shifted radially by 2.5 mm. This is the difference between two curves in Fig. 7.

causes large currents and large restoring forces respectively. Fig. 9 shows the distribution of the eddy currents within one quarter of the conducting disk at 15,000 RPM and 2.5 mm disk displacement. Fig. 10 shows the axial distribution of the magnitude of the eddy current density at 35 kRPM. For the 12.7mm-thick disk, significant current flows throughout the entire cross-section of the disk.

In the unrolled model, the eddy current in the conductor has some phase shift with respect to the excitation. This phase shift differs from one point of the conductor to another. When performing frequency analysis, FEA returns real and imaginary parts of the eddy currents in each point of the conductor, from which the amplitude and phase of the current can be calculated. Integrating the cross-product of the eddy current density and axial magnetic flux density over the volume of the disk we were able to obtain the magnitude of Ampere's force acting on the conductor as well as its phase with respect to the excitation field. When converting from the unrolled model back to the original rotational system, the phase shift between the force and the excitation field converts into an angle in space between the force and the displacement. Figs. 11 and 12 show the magnitude of the in-plane radial stiffness (ratio of the net force vs disk displacement) and the angle between the force and the displacement as functions of the rotational speed. The angle between the force and the displacement has a negative effect on the system performance: higher angles require more damping to achieve stability.

When the hub thickness increases, the axial distribution of

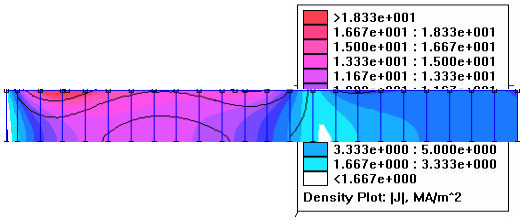


Fig. 9. Distribution of the eddy currents within one quarter of the disk cross-section at 15 kRPM and 2.5 mm displacement.

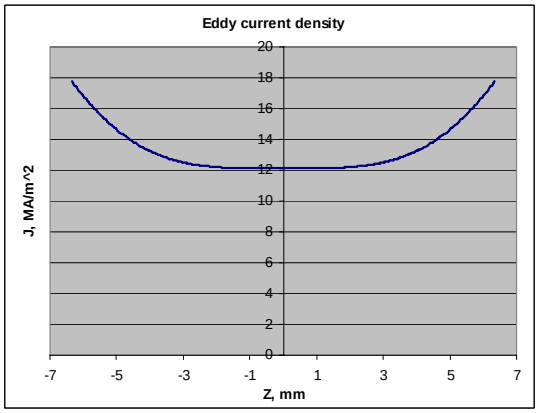


Fig. 10. Variation of the induced current magnitude through the thickness of the 12.7mm-thick aluminum disk between the poles at 35 kRPM.

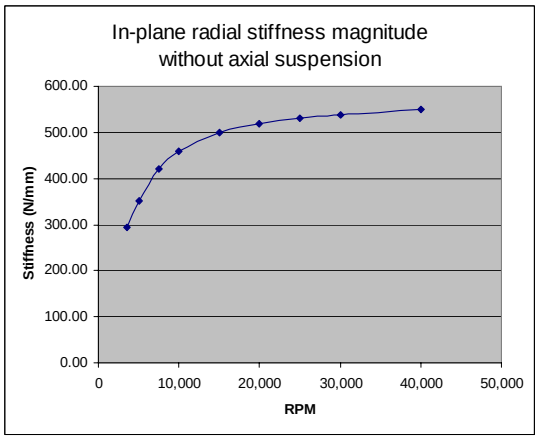


Fig. 11. In-plane stiffness (ratio between the magnitudes of the force and displacement) as a function of the rotational speed of a 12.7mm-thick disk displaced by 2.5 mm.

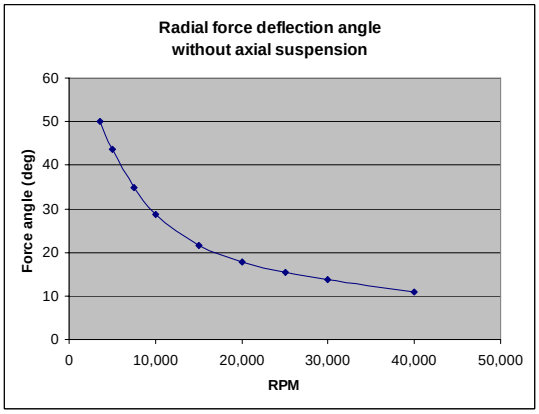


Fig. 12. Angle between the force exerted on the aluminum 12.7mm-thick disk and the disk displacement as a function of the rotational speed.

the field inside the hub becomes non-uniform. Fig. 13 shows such a distribution calculated for the middle section of one of the poles for the 96mm-thick hub (compare with Fig. 6 for the 12.7 mm hub). Furthermore, because of the skin-effect at high rotational speeds, the current flows only in a relatively small portion of a thick hub adjacent to its

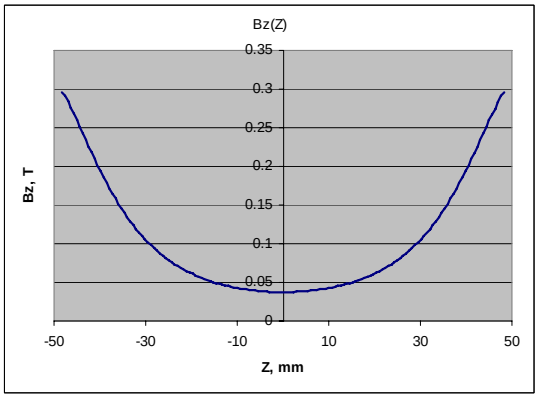


Fig. 13. Distribution of the axial field component through section of the 96mm-thick disk in the middle plane of one of the poles.

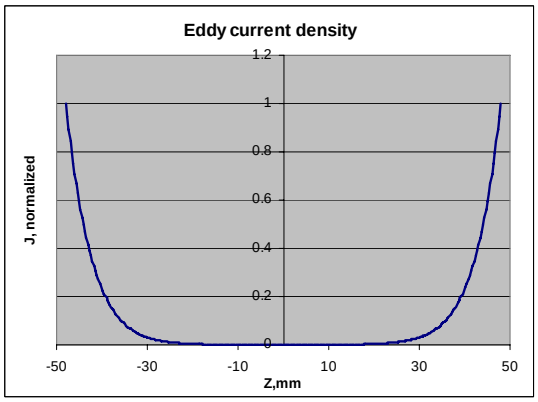


Fig. 14. Variation of the induced current magnitude through the thickness of the 96mm-thick aluminium disk between the poles at 35 kRPM.

surface. Fig. 14 shows the shape of the induced current density throughout the thickness of the hub at 35kRPM (compare with Fig. 10 for the 12.7mm hub).

The calculation of the electromagnetic forces acting on the 96mm-thick hub becomes more complicated than for the 12.7mm-thick disk because the field distribution is non-uniform in the z direction. This calculation was performed at only one speed – 35 kRPM. The estimated electromagnetic stiffness at this speed was 210 N/mm. (For the 12.7mm-thick hub the stiffness at the same speed was approximately 543 N/mm, see Fig. 11). This stiffness is believed to be adequate for applications which do not experience significant radial loadings. This is typically the case in space-born and stationary Earth-based systems operating vertically.

- Introducing radial damping

The non-contact equilibrium of a conductor rotating in a circumferentially uniform magnetic field is always unstable, however, this instability can be compensated with radial damping [2-4]. Ignoring the effects due to the axial suspension and assuming that the motion occurs in a single plane, the amount of damping necessary for stability at speed ω is

$$C(\omega) = \sqrt{mK(\omega)}\,\frac{\sin(\theta(\omega))}{\sqrt{\cos(\theta(\omega))}} \qquad (1)$$

where $m$ is the rotor weight, $K(\omega)$ is the in-plane suspension stiffness, and $\theta(\omega)$ is the cross-coupling angle. Fig. 15 shows how much of radial damping is needed to achieve stability in the system with 96-mm hub.

No axial suspension has been assumed so far. The introduction of a passive element that produces a positive axial stiffness will result in the negative (destabilizing) radial stiffness $K_{des}$ [2,3]. This negative stiffness subtracts from the radial component of the in-plane stiffness due to the interaction of the disk with the stationary field, without affecting its tangential component. As a result, both the magnitude and the direction of the net in-plane radial stiffness are changed. The upper curve in Fig. 15 is obtained with an assumption that the axial suspension introduces $K_{des}$ =-70 N/mm. This corresponds to a positive axial stiffness of ≈ 140N/mm. The rotor weight is assumed to be 68 kg in both cases. More damping is needed for stability in the presence of the passive axial suspension.

While a fully passive system is feasible, an active damper is found to be advantageous due to significantly lower weight. A possible active damper actuator design is shown in Fig. 16. If the ends of the damper windings were simply shorted, the damper would work in a passive mode without external electronics. Two dampers located on two sides of the flywheel will produce 244 Ns/m damping coefficient in this case. According to Fig. 15, for the suspension to be stable at 15 kRPM, a damping coefficient in excess of 2000 Ns/m is required. This can be achieved by connecting the damper windings to simple electronic circuits described in [3]. A ten-fold damping coefficient increase has been demonstrated practically using this approach.

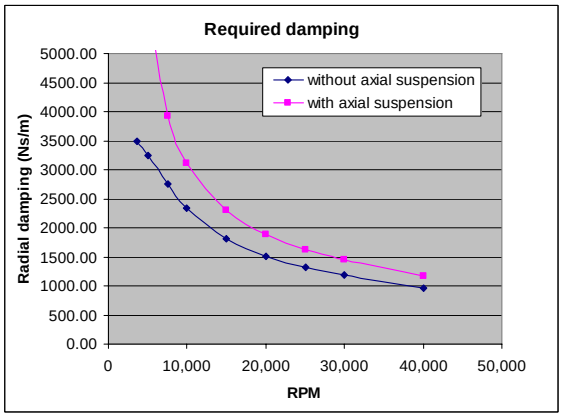


Fig. 15. Minimum amount of radial damping required for the stability of the system with the 96mm-thick hub as a function of speed. 140 N/mm axial suspension stiffness is assumed

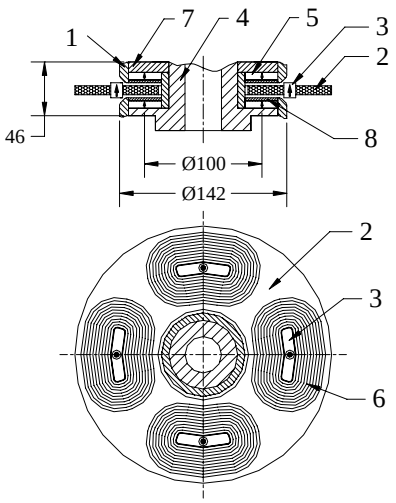


| | | | |
|---|---|---|---|
| **1** | Restraining sleeve (Inconel) | **5** | Permanent magnets of the radial damper (NdFeB) |
| **2** | Active damper stator | **6** | PCB windings |
| **3** | Axial suspension stationary magnet (NdFeB) | **7** | Back-iron (Hiperco 50 or soft-magnetic steel) |
| **4** | End shafts (Hiperco 50 or soft-magnetic steel) | **8** | Damper pole shoes (soft-magnetic steel) |

Fig. 16. A possible design of an active radial damper.

- Thermal stability

The most critical component of the system from the thermal prospective is the aluminium hub, which might carry significant eddy currents while spinning in a vacuum where the heat removal is limited to radiation. The power dissipation in the disk can be calculated as

$$P = K\sin(\theta)\Omega d^2 \qquad (2)$$

where $K$ is in-plane radial suspension stiffness, θ is the force-displacement cross-coupling angle, Ω is the spin velocity in rad/sec, and $d$ is the radial disk displacement from the equilibrium position. At 35 kRPM and 0.25 mm displacement, the heat dissipation in the 96mm-thick hub will be approximately 12 W. FEA thermal analysis shows that the equilibrium temperature of the hub dissipating this power will be only 20°C above the containment temperature.

Another positive factor is a large specific heat capacity of the aluminium - C=900 J/(kg·°C) – the highest among commonly used metals. The amount of time needed to increase the temperature of the 50 kg hub by ΔT=20°C due to 12 W power dissipation without any radiation will be

$$t = \frac{Cm\Delta T}{P} = 75000\,\text{sec} = 21\,\text{hour}$$

### *D. Axial and Angular Suspensions*

Positive axial stiffness is introduced utilizing the interaction between the rotating magnets *5* (Fig. 16), also used in the damper, with stationary magnet segments *3*. Positive angular stiffness is achieved by using two pairs of mutually attractive magnets located at the far ends of the rotor (Fig. 1). Because of the large distance between the magnets, relatively low linear interaction stiffness results in large angular stiffness. The final values of the net stiffnesses and damping coefficients in the system with 96mm-thick hub are as follow:

Radial and axial stiffness: 140 N/mm
Angular stiffness: 1100 N·m/rad
Radial damping: 2000-6000 N·s/mm
Angular damping: 26-78 N·m·s/rad

### *E. Permanent Magnet Motor/Generator.*

An axial-flux ironless permanent magnet motor-generator has been preliminary selected for the LEO satellite applications. Low output power requirements (4 kW) resulted in a small size of the machine. The main criterion for the selection was to minimize negative stiffness introduced by the motor/generator. The design details are outside the scope of this paper.

## III. CONCLUSION

The possibility of using homopolar electrodynamic magnetic bearings for FESS applications has been evaluated using an example of a FESS for LEO satellites. Some of the major advantages of this technology, also discussed for example in [1-4], include:

- Simpler design compared to AMB
- Negligible power rating and complexity of the associated electronics
- Easy implementation of the high degree of the redundancy of the electronics
- No position sensors
- Gentler failure modes compared to AMB due to positive stiffnesses in all directions at high speeds
- Low rotational losses

A 2.6kWh 6.4kW FESS for LEO satellites utilizing homopolar electrodynamic magnetic bearings has been found feasible based on preliminary electromagnetic, stress, rotordynamic and fatigue analyses.

## REFERENCES

[1] C. Murakami, I. Satoh, “Experiments on a very simple radial-passive magnetic bearing based on eddy currents”, ISMB7, August 2000, Zurich, pp. 141-146.

[2] A. Filatov, E. Maslen, G. Gillies, "A method of noncontact suspension of rotating bodies using electromagnetic forces", Journal of Applied Physics, Vol. 91, pp. 2355-2371, 2001.

[3] A. Filatov and E. Maslen, “Passive magnetic bearing for flywheel energy storage systems”, IEEE Trans. Magn., vol. 37. no. 6, pp. 3913-3924, 2001.

[4] T. Lembke, “3D-FEM analysis of a low loss homopolar induction bearing”, ISMB9, August 2004, Lexyngton, KY.

[5] K. Davey, A. Filatov, R. Thompson, “Design and analysis of passive homopolar null flux bearings”, IEEE Trans. Magn., vol. 41. no. 3, pp. 1169-1175, 2005.

[6] Flywheel Energy Systems Inc., “Development of high performance flywheels for electromechanical batteries”, Contract No. 23440-4-1191/01-SQ Final report, March 1997.

[7] S. Earnshaw,“On the nature of the molecular forces, which regulate the constitution of the luminiferous ether,” Transactions of Cambridge Philosophical Society, vol. 7, pp. 97–112, 1842.

[8] W. Braunbek, “Freischwebende korper im elektrischen und magnetischen feld” *Z. Phys.*, v ol. 112, pp. 753–763, 1939.